Development of Test Rig for Position Control of Shape Memory Alloy Springs using PID Algorithm.

Author

Shozib Mahmood Bhutta

Registration Number

2017-NUST MS DME-205684

Supervisor

Dr. Mushtaq Khan

DESIGN AND MANUFACTURING ENGINEERING DEPARTMENT

SCHOOL OF MECHANICAL & MANUFACTURING ENGINEERING

NATIONAL UNIVERSITY OF SCIENCES AND TECHNOLOGY

ISLAMABAD

JUNE 2021

Development of Test Rig for Position Control of Shape Memory Alloy Springs using PID Algorithm.

Author

Shozib Mahmood Bhutta

Registration Number

2017-NUST MS DME-205684

A thesis submitted in partial fulfillment of the requirements for the degree of

MS Mechanical Engineering

Thesis Supervisor:

Dr. Mushtaq Khan

Thesis Supervisor's Signature: _____

DEPARTMENT OF DESIGN AND MANUFACTURING ENGINEERING

SCHOOL OF MECHANICAL & MANUFACTURING ENGINEERING

NATIONAL UNIVERSITY OF SCIENCES AND TECHNOLOGY,

ISLAMABAD

JUNE 2021

Thesis Acceptance Certificate

It is certified that the final copy of MS Thesis written by **Shozib Mahmood Bhutta** (Registration No. **205684**), of Department of **Design and Manufacturing Engineering** has been vetted by undersigned, found complete in all respects as per NUST statutes / regulations, is free from plagiarism, errors and mistakes and is accepted as a partial fulfilment for award of MS Degree. It is further certified that necessary amendments as pointed out by GEC members of the scholar have also been incorporated in this dissertation.

Signature: _____

Date: _____

Dr. Mushtaq Khan (Supervisor)

Signature HOD: _____

Date: _____

Signature Principal: _____

Date: _____

FORM TH-4

MASTER THESIS WORK

We hereby recommend that the dissertation prepared under our supervision by: **Shozib Mahmood Bhutta 2017-MS DME-205684.** Titled: **Development of Test Rig for Position Control of Shape Memory Alloy Springs using PID Algorithm** be accepted in partial fulfillment of the requirements for the award of **MS** degree.

Examination Committee Members

1. Name: **Dr. Syed Hussain Imran** Signature: _____

2. Name: **Dr. Najmul Qadir** Signature: _____

3. Name: **Engr. Haroon Ahmad Khan** Signature: _____

Supervisor's name: **Dr. Mushtaq Khan** Signature: _____

Date: _____

_____ _____

Head of Department Date

COUNTERSINGED

Date: _____ _____

Dean/Principal

Declaration

I certify that this research work titled "*development of test rig for position control of shape memory allow springs using PID algorithm"* is my own work. The work has not been presented elsewhere for assessment. The material that has been used from other sources it has been properly acknowledged / referred.

Signature of Student

Shozib Mahmood Bhutta

2017-NUST-MS DME-205684

Plagiarism Certificate (Turnitin Report)

This thesis has been checked for Plagiarism. Turnitin report endorsed by Supervisor is attached.

Signature of Student

Shozib Mahmood Bhutta

2017-NUST-MS DME-205684

Signature of Supervisor

Dr. Mushtaq Khan

Copyright Statement

- Copyright in text of this thesis rests with the student author. Copies (by any process) either in full, or of extracts, may be made only in accordance with instructions given by the author and lodged in the Library of NUST School of Mechanical & Manufacturing Engineering (SMME). Details may be obtained by the Librarian. This page must form part of any such copies made. Further copies (by any process) may not be made without the permission (in writing) of the author.
- The ownership of any intellectual property rights which may be described in this thesis is vested in NUST School of Mechanical & Manufacturing Engineering, subject to any prior agreement to the contrary, and may not be made available for use by third parties without the written permission of the SMME, which will prescribe the terms and conditions of any such agreement.
- Further information on the conditions under which disclosures and exploitation may take place is available from the Library of NUST School of Mechanical & Manufacturing Engineering, Islamabad.

Acknowledgement

All praises to the Almighty Allah, who gave me the strength to embark on the momentous journey of my career and the courage I needed to complete this work. Without the blessings of the Rahman our lives have no meanings.

I thank my supervisor Dr. Mushtaq Khan for the effort and believe he put in me to complete this research. The motivation he instilled in me has been a great help during this work. I thank him not only for his professional help but also for the words of wisdom he offered me during testing times.

I would also like to extend my gratitude towards the members of the Guidance and Examination Committee of Dr. Najam-ul-Hassan, Dr. Hussain Imran and Engineer Haroon Ahmad Khan. They were helpful throughout the process and always welcomed my questions with great interest.

I would like to thank my friends who were always my support during the whole master's program. They helped me during difficult times to stay positive and take the challenges head on.

Saving the best for the last, I thank my parents for their undying love towards me. They have been my biggest inspiration and best friends. I am grateful to my brother for being a caring and loving influence.

Author

Dedicated to my exceptional parents and adored siblings whose tremendous support and cooperation led me to this wonderful accomplishment.

Abstract

Shape memory alloys are special materials which memorize their original form. These can be brought back to their programmed state after deformation by virtue of heat or magnetic stimuli. Nitinol or Nickle Titanium Alloy (NiTi) is the best known SMA. A great amount of research has been done in order to understand their chemical composition and physical properties. These materials have applications ranging from aircrafts to miniature robots and are used in medical field due to their unique behavior. SMAs offer a unique perspective in the micro-positioning industry where they can replace bulky machinery like motors to move small objects around using only heat supplied through electric current. As of now, the research is focused on controlling SMA position using complex algorithms designed in labs and the industrial application is very limited. This thesis describes the use of simple PID and Advanced PID algorithm, that can be implemented in industry, to control the position of Nitinol springs. The research carried out indicates that, although difficult, the PID algorithm can produce good results. The PID controller reached an accuracy of 0.46mm with a minimum overshoot of 1.8344mm while the advanced PID gave a minimum error of 0.211mm and the minimum overshoot at 2.38mm.

Key Words: *Nitinol, Shape Memory Alloys, Position Control, PID algorithm*

Table of Content

List of Figures

List of Tables

CHAPTER 1: INTRODUCTION

A lot of improvement in technology is observed at a rapid rate. There is a motivation in industry to move from conventional mechanical actuators to more light weight electrically controlled actuators. This move has inspired researchers to investigate the potential that is offered by Shape Memory Materials (SMMs). Shape Memory Materials have a special ability to remembering/retaining their shape even after deformation occurs. The memorized shape can be recalled using thermal/magnetic stimuli.

Shape Memory Alloys are a class of SMMs which contain a combination of different ferrous/non-ferrous materials synthesized in a way to allow them to memorize a pre-determined shape. SMAs are categorized as following:

1. Ferrous SMAs
2. Non-Ferrous SMAs

Ferrous Shape Memory Alloys contain Iron (Fe) as the main component of material structure. These Alloys can be actuated/stimulated using mainly electromagnetic forces due to the presence of Iron. One such example is Fe-Mn-Si

Non-Ferrous SMAs are composed of materials other than Iron. These respond mainly to thermal stimulus to bring them back to their pre-determined shape. These include Nickel and Copper based alloys etc. Some examples include Nickel Titanium Alloys Ni-Ti, Copper-Zinc-Aluminum Cu-Zn-Al, and Copper-Aluminum-Nickel Cu-Al-Ni

Nitinol-Ni-Ti is one such example of non-ferrous SMAs which is widely used for experimentation purposes related to actuation and displacement. Nitinol has unique properties which makes them superior to other SMAs. The iron and copper based SMAs that are widely available and cheap as compared to Nitinol, but they offer poor thermomechanical properties, and are unstable as compared to Ni-Ti.

Shape Memory Alloys exhibit two inherent properties:

1. Shape Memory Effect
2. Super-elasticity

Shape Memory Effect is the property by which the SMAs are brought back from a deformed state to the original state i.e., the preset shape by the stimulus of temperature or electromagnetic forces. This property is useful when working with position control systems and actuators.

Super-elasticity as the name suggests is the ability of SMAs to become exhibit very high elasticity in normal temperatures. This property is useful in creating durable products like frames of sunglasses and other useful products.

The SMAs have their special ability due to their unique structural arrangement. These structures are:

1. De-twinned Martensite

2. Twinned Martensite
3. Austenite

The **Detwinned martensite** is the normal structure when no external loading is applied. The **Twinned Martensite** is generated when external loading is applied on the SMA and is deformed to a new shape. The **Austenite** structure is observed when the temperature of the shape memory alloy reaches above the phase change/transition temperature and the shape of SMA is restored to the original.

1.1. AIM

For SMA springs the amount of research is relatively small because of some disadvantages including the strain that is built up after repeated use. It has been observed that after repeated cycles the elasticity of SMA springs in normal (martensite) state is reduced considerably. The aim of this research is to find the relationship between current and displacement produced as a result of actuation process and to control the micro-positioning of SMA spring using a PID algorithm with a goal to minimize the error.

1.2. Objectives

1) Developing a testing rig to analyze the properties of SMA springs under study
2) Determining best Duty Cycle (DC) and input voltage for optimal actuation process
3) Determining the relationship between displacement and Duty Cycle of PWM at a given voltage
4) Determining the maximum load that can be lifted by SMA spring at optimal Duty Cycle and Voltage
5) Determining the relationship between Current and Displacement using LVDT for precise reading
6) Implementing a control mechanism using PID for accurate micro positioning

1.3. Research Methodology

The goal of this research was to create an experimental rig and software to observe best operating voltages, load bearing capacities, LVDT displacement measurements, PID and advanced PID controls for accurate positioning of SMA springs.

First a literature review is conducted to understand the properties and behavior of SMA alloys. The loading capacity, thermoelectric behavior and hysteresis is studied. A review of control mechanisms for the positioning of SMAs is also considered. Previous research carried out to explore the unique performance of Nickel-Titanium Alloys (Nitinol) is also studied. The micro-positioning of shape memory alloy wires and springs, with different techniques and variables applied, is also discussed in this review.

Based on the literature review a testing rig is developed to test the performance of Nitinol springs. The rig consists of two platforms to support the movement of SMA wire along with the dead weights which hang on the spring. Position sensing devices like LVDT and HC-SR04 are incorporated to measure displacements.

A software development phase is introduced in the thesis to give background on how to perform different experiments. The programs are developed in LABVIEW 2017 which is a great platform to interact with sensors and give output to the physical hardware. This gives a lot of freedom to try several combinations for any experiment that needs to be performed.

1.4. Thesis Outline

The thesis is divided into Introduction, Literature Review, Experimental Setup design, Software development and Results of Experiments.

Chapter 1 is the introduction which gives an overview of the research carried out, its goals aims, and methodology implemented.

Chapter 2 gives a detailed background research into the Shape Memory Alloys and their properties. The research carried out in the past. The inspiration and expertise gained from the previously presented results, based on which the current experiments were performed.

Chapter 3 deals in the experimental design of the testing rig used to perform experiments. The components used; the platform created; and hardware integration.

Chapter 4 discusses the software developed to perform experiments and different variations of program used to get various results.

Chapter 5 is a discussion on the results generated, data collected and interpreted as a result of performing the experiments.

Chapter 6 is the conclusion of the research which discusses the results and future recommendations resulted from this research.

CHAPTER 2: LITERATURE REVIEW

2.1. Introduction

The advancement of technology in the field of smart structures and materials is moving at a rapid pace. There has been an inclination of industry for moving towards light weight actuators that can replace traditional bulky mechanical equipment. Especially in the automotive sector, most of the actuators like cams in the engine require a lot of work to be rotated. The idea is to replace these with smart materials that can be timed using electrical signals. However, a lot of work is required to bring this technology into practical use.

SMAs were first discovered by a Swedish Physicist Arne Olander in 1932. Olander noticed that gold-cadmium (Au-Cd) alloy regained its shape by heated after being deformed. Similar effects were discovered in copper-zinc (Cu-Zn) and copper-tin (Cu-Sn) alloys by Greninger and Mooradian, and the name Vernom in 1941 gave the name “Shape Memory” to the materials exhibiting such properties. SMAs came under light in 1960 when Nickle-Titanium (Ni-Ti) were discovered, these were named Nitinol which gave importance to these materials and the research continues to this day [1]. The SMAs provide an exciting opportunity to transform industry which towards material saving, miniature robotics, mini-linear actuators applied in almost all industrial applications and the future transformation of technology[2].

Since the discovery of Nitinol, Shape Memory Alloys have been researched extensively to make their way into the commercial market. SMAs have gained a lot of success in the medical field with a result of higher life expectancy and reliability of medical equipment produced. The two most common equipment are stents and dental implants[3]. In non-medical fields the use of SMAs as actuators, super-elastic materials etc. is also growing rapidly because of the ability of SMAs to be tuned to the specific application need[4].

There are still a few limitations as there is less information available on the recovery stresses, wear resistance, fracture mechanics etc.[4], which makes the widespread use of SMAs less common. Studies are being carried out to better understand their characteristics. Computational studies are being conducted to model these materials for different applications, one such study successfully compared the computational model with experimental results for biomedical applications[5].

For the actuation process the research is continued on how to use SMAs to gain precise positioning during such applications. A selection mechanism has been devised by W. Huang et.al for various actuator applications comparing Nitinol, Cu-Zn-Al, and Cu-Al-Ni using charts and tables [6]. The most work, apart from medical applications, carried out is for the accurate micro-positioning employing different techniques like modulated adaptive controller[7], neural network-based controller[8], PID algorithms[9] etc. The model-based systems such as Inverse Hysteresis, Neural Networks etc. have limited industrial applications because of complex physical models and hard to understand theoretical controllers[10].

2.2. Shape Memory Alloys

Shape memory Alloys are special materials which can memorize a pre-defined shape, hence the name Shape Memory. These Alloys come back to their original shape after deformation when stimulated by heat or electromagnetic signals.

2.2.1. Types of SMAs

SMAs can be classified into:

1. Ferrous SMAs
2. Non-Ferrous SMAs

Ferrous Shape Memory Alloys have iron as the base component and because of that are actuated by electromagnetic stimulus.

Non-Ferrous Shape Memory Alloys do not have iron as the base component. These are stimulated, generally, through heat. Examples of these are Copper based SMAs and Nickle Titanium shape memory alloys.

2.3. Advantages of Shape Memory Alloys

Shape Memory Alloys are light weight and strong materials. These can make good actuators replacing a lot of bulky mechanical structures and pneumatic assemblies. Jan Van Humbeeck et.al have discussed many applications from fashion and gadgets, couplings and fasteners, to micro-actuators and smart structures[4].

Nickel Titanium SMAs have been a blessing for the medical industry. Their applications are consistently increasing. N.B. Morgan and colleagues discuss these applications in much detail ranging from Nitinol guidewires, Stents, Stent grafts, to many clinical instruments and orthopedic applications[3]

2.4. Limitations of Shape Memory Alloys

Although SMAs are part of a revolutionary discovery, these still have many limitations. These are needed to be overcome to make way for the widespread applications. Some of these are:

- Narrow Bandwidth, which makes it difficult for SMAs to dissipate heat quickly.
- Small Strain life, under fatigue testing, the strain life of SMAs decrease consistently as the number of cycles increase[11]
- Low actuation frequency
- Low controllability
- Low Accuracy
- Low Energy Efficiency

2.5. Structure of SMAs

Unlike many materials SMAs have a non-linear path while moving from one state to another. Shape memory Alloys have three basic structures[12] which are responsible for their unique properties. These are:

1. Twinned Martensite
2. Detwinned Martensite
3. Austenite Structure

The material changes its structure as the temperature/electromagnetic stimuli varies. SMAs have two phases under which the transformation takes place:

1. Martensite Phase
2. Austenite Phase

The SMAs exist in Martensite Phase at low temperatures and in Austenite Phase at high temperatures. The temperature range varies material to material and by the tuning process to transform at a certain *transition temperature*[13]. The phase transformation is better explained by the figure below.

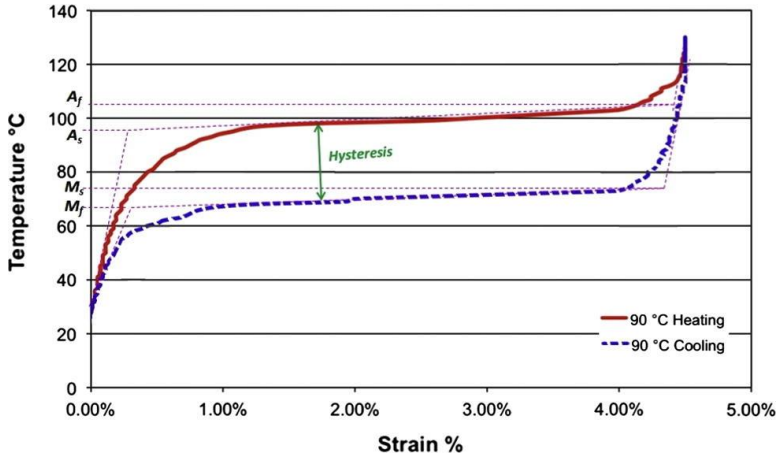

Figure 1 SMA Phase Transformation[1]

When the Shape Memory Alloy (SMA) is heated the transition from martensite to austenite phase starts at Austenitic start temperature $\mathbf{A_s}$. The transformation gets completed at the Austenitic finish temperature $\mathbf{A_f}$. Heating the SMA further changes its properties until a temperature $\mathbf{M_d}$ is reached where anymore heating does have any effect on the structure of the material. Similarly, during the cooling process the transformation from Austenite to martensite takes place from Martensite start temperature $\mathbf{M_s}$ and finishes at Martensite finish temperature $\mathbf{M_f}$[14]**.** There is a difference between heating and cooling transition curves is termed as ***hysteresis,*** which shows the amount of heat/work lost during the heating process. The structural transformation is best explained in the figure below:

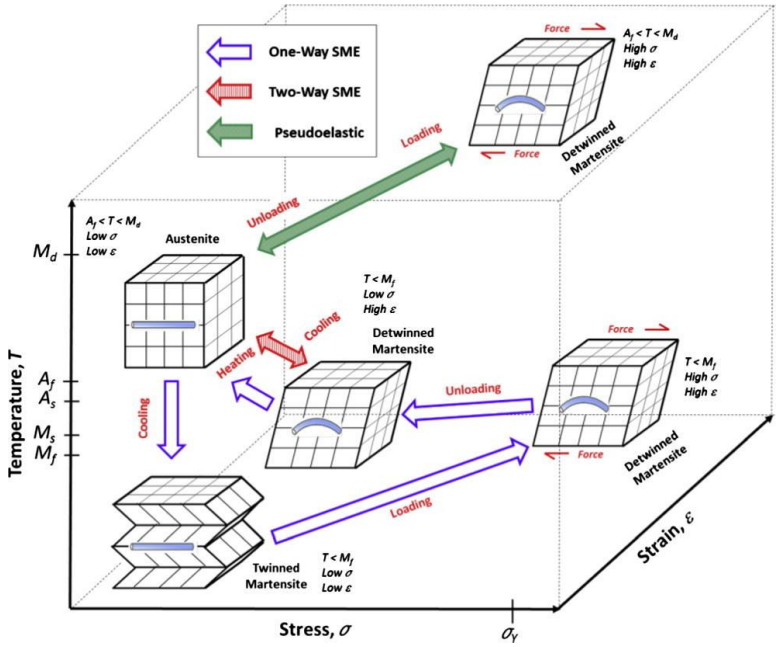

Figure 2 Structural Transformation in SMAs[1]

2.6. Shape Memory Effect and Super-Elasticity

Shape Memory Effect (SME) is the property of SMA to regain its original form by heating after it has been deformed. SME is a reversible process which is characterized as:

- One-Way Shape Memory Effect: The SMA keeps the deformation after the load is removed and re-arranges itself back when heated above transition temperature.
- Two-Way Shape Memory Effect: The SMA retains/remembers its shape at both high and low temperatures.

One-way SMAs are much common in application compared to two-way SMAs. Two-way SMAs provide half the recovery strain compared to one-way SMAs and are difficult to train/tune.

Super-elasticity also called pseudo-elasticity is the property of SMAs to retain their state when stress is removed in Austenitic phase. This property is observed at temperature between $\mathbf{A_f}$ and $\mathbf{M_d}$. For such SMAs the transition temperature is usually kept very low to use this property in normal conditions.

2.7. SMA Actuators and control

The potential of Shape Memory Alloys being used as actuators is sought out increasingly in the industry. SMA actuators have power density higher than hydraulic actuators. Reynaerts & Van Brussel et al defined a number of rules to follow for designing SMA based robotic actuators, explaining the attraction of such actuators in especially space and zero gravity environments and the optimal cooling methods to obtain optimal position control[15].

Such properties are very attractive in industrial applications. There is a huge potential of replacing bulky mechanical actuators with lightweight electrically actuated SMAs. Because shape memory alloys have a non-linear path of transformation. Their control becomes difficult due to the hysteresis phenomenon[16]. A study published by Yee H. The and Roy Featherstone determined the first order transfer function relating heating input to output force on the SMA wires using magnitude and phase responses helping to understand and position control of actuators[17]. Such research can be the foundations for the most sought out goal regarding smart materials i.e. the micro-positioning applications.

Position control/micro-positioning is the most research field in SMA. Research is being carried out to find a simple solution that can be applied in widespread applications. A self-sensing model using PID and Fuzzy logic controls is improved by Sang Hak Lee and Sang-Woo Kim which provides an applicable solution for position control of SMAs[18]. For the time being, the practical use of precise positioning actuators is limited. Most of the research deals with sophisticated techniques which are difficult to apply in large scale applications.

2.8. Pulse Width Modulation

Since a lot of research is carried out on shape memory alloy wires, alternate current (AC) is used to supply current and heat the wire using Joule's heating phenomenon. In this research the Nickle Titanium Alloy (Nitinol) spring is used as an actuator and is a coil through which AC cannot pass through. Instead, a Direct current (DC) source is used to as a supply to the circuit.

A DC input can damage the SMA wire and needs to be controlled when passing through the SMA springs. For this purpose, a technique called Pulse Width Modulation (PWM) is used to safely operate the spring without damaging the material. PWM implies that the current shall be passed through in pulses of on/off instead of a straight maximum voltage. It is defined as a percentage value of the current input to the circuit. For example, the 50 percent PWM value gives current in pulses when the input will be on only half of the time, whereas a 100 percent PWM supply means that the maximum current passes through without any off time i.e., no pulses.

2.9. PID Algorithm

PID algorithm is used extensively in real world applications such as control of water levels in a tank, temperature control inside a boiler, or pressure levels in a pipe of hot gases. It uses three levels of control structure to monitor and change the input. These are Potential, Integral and Derivative control.

Potential control is a linear control which subtracts the desired value from real value and gives an error to the system which then adjusts to reach the desired value.

Integral control uses the integration of real values over time and suggests the pace of adjusting to reach the desired point based on the historic data of change in values.

Derivative control uses time derivatives of the real values overtime to find out the speed of change. It suggests the rate at which the values should change in order to reach and stay at the desired value of output.

The most common algorithm used in the industry is the PI algorithm which combines the potential and integral values to remain within the tolerable range of desired values needed for smooth operation. In essence, PID simply returns errors based on the input it is getting and feeds these errors into the system which corrects itself based on the results. PID systems need to be tuned to integrate in a system and tested before the start of operation. Different techniques are being developed to make use of PID in a robust and efficient way so that they can be integrated like a “plug and play” tool. Kiam Heong Ang and Gregory Chong describe an overview of techniques and functionalities of modern PID algorithms and their tuning processes used in different software tools and patented technologies[19].

The goal of this thesis was to use different easily applicable techniques to monitor and understand the position control of Nitinol spring actuator. Different PID tuning methods were implemented to move closer to frequent use of such materials in precision industry.

CHAPTER 3: EXPERIMENTAL SETUP

For testing the performance of the SMA springs a testing rig was designed as shown in the figure below. The design was inspired by several experiments carried out in previous research on the SMA wires. The idea is to examine the capability of spring to return to its original state under different loads with varying voltage and current inputs.

3.1. Testing Rig

The rig consists of three platforms. The top platform has a hook attached at the center. The hook is used to hang the springs with weights attached at the bottom.

The bottom platform has an LVDT (Linear Variable Differential Transformer)/Displacement Sensor, fixed with the help of silicone gel, which is responsible to detect the displacement produced by the spring. The middle platform contains a hole in the center which allows the LVDT and SMA spring to connect. In addition, a hollow tube is used to capsule the spring as to limit the oscillatory motion caused by the displacement of spring. The top of the platform has a hook attached to the center of the plate to allow springs/wires to hang for the experiments to be carried out. The top plate is adjustable to allow variable heights at which the weights can be hanged. Threaded rods, 10mm in diameter, are used as supports to the platforms which help to balance and to reposition them in comparison to one another. This action of changing the position of platforms is carried out with nuts which are tightened whenever an experiment is carried out to make sure there are no errors in displacement caused by outside forces.

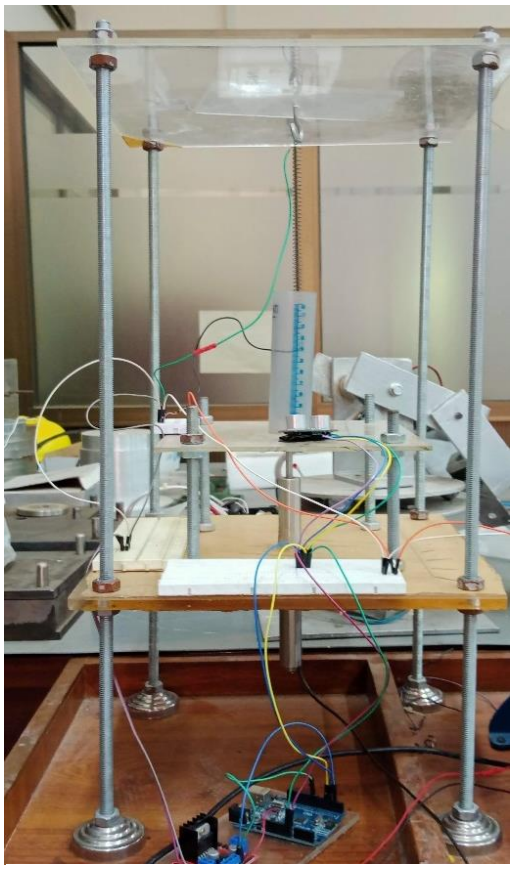

Figure 3 Testing Rig

There are different sensors attached to the rig that are used to gather important data for the success of this thesis. Different devices are used to provide current to the spring and control the movement. The rig is designed in a way that allows the height to be varied, which allows different weights to be attached to the spring. This in turn helps accommodate the increase in elongation caused by the heavier loads. The electric connections are setup using jumper cables and bread boards which makes the electric interface modular in design and different connections can be made depending on different experimental procedures.

3.2. SMA Springs

SMA springs used in this experiment are procured from a renowned Nitinol supplier by the name of Kellogg's Research Labs. The spring is unique in its properties as discussed in the introduction and literature review.

Figure 4 Shape Memory Alloy Spring

The specification of springs are as follows:

Wire Size	0.5 mm (0.020 inch)
Spring Length	50.8 mm (2 inches)
Mandrel Diameter	6.3 mm (0.250 inch)
Pitch	2x wire size
Transition Temperature	45^{o}C

3.3. LVDT Sensor

A position sensor is used to accurately measure the position of nitinol wire when stimulated with electricity. The sensor is called Linear Variable Displacement Transformer (LVDT). The device is highly sensitive and gives precise reading for any movement/displacement.

Figure 5 Linear Variable Displacement Transducer (LVDT)

The general specifications of an S-series LVDT are as follows:

Description	LVDT Variants	Range
Storage Temperature	40-20 mA DC variant	-20°C to 85°C
Operating Temperature	4-20 mA DC variant	0°C to 65°C
Linearity	0.2%FSO	

Table 1 S-series LVDT general specifications

The transducer relies on magnetic flux for measurement. Any small change in the displacement sends an electrical signal to the computer and hence the sensor has virtually infinite resolution. The LVDT used here is an S-series transducer. It has a maximum stroke length of 50mm, the outer diameter is 19mm. A spring is attached to the core which helps as a guide and keeps the core extended to the movable plate.

3.3.1.Electrical Interface of LVDT

A DC voltage LVDT is used in the test rig. The output is a DC voltage which is then converted to displacement according to the table given in guidelines.

Measurement Range	Output Voltage
0-d mm	0 to 5 V
-d/2 to d/2 mm	-5 to 5 V

Table 2 Voltage to Displacement conversion

3.3.2.Calibration of LVDT

A chart is provided by the manufacturer to help in the process of calibration. The calibration is done on LABVIEW 2017 before implementing the LVDT in the testing rig. The calibration chart is shown below:

Position (mm)	Output(V)	Error (%FSO)
-25.000	-4.9907	-0.093
-20.000	-3.9939	-0.061
-15.000	-3.0012	0.012
-10.000	-2.0047	0.047
-5.000	-1.0080	0.080
0.000	-0.0030	-0.030
5.000	1.0023	0.023
10.000	2.0024	0.024
15.000	3.0055	0.055
20.000	4.0001	0.001
25.000	4.9999	-0.001

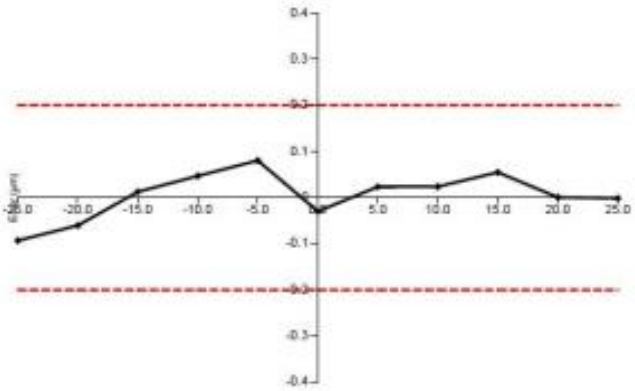

Figure 6 Calibration Chart LVDT

3.3.3.Electric Circuit of LVDT

The circuit by which the connections are made in the test bench is shown below:

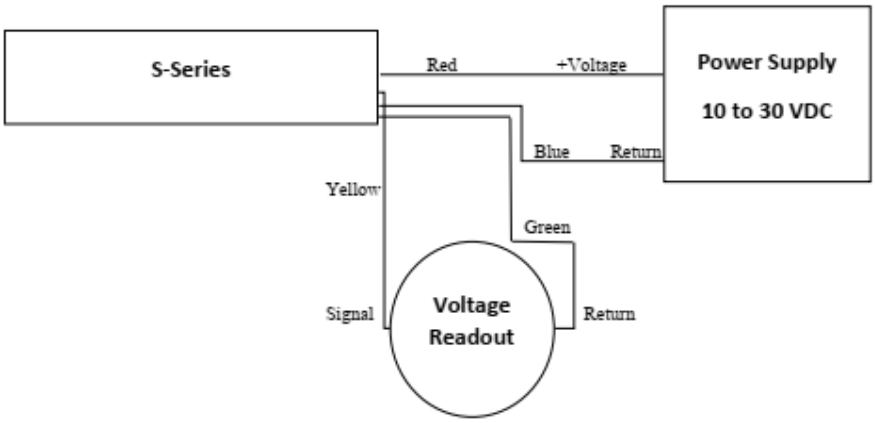

Figure 7 Electric Circuit for LVDT Installation

3.4. HC-SR04 Position Sensor

Ultrasonic ranging module HC-SR04 is a non-contact position sensor with a range between 2cm-40cm with an accuracy around 3mm. This module uses ultrasonic sound signals to measure the distance from its center to an object directly Infront. This is used in the experiment for initial readings to test the load bearing capacity of spring at different voltages.

Figure 8 HC-SR04 Position Sensor

3.5. Data Acquisition Hardware

Data gathering devices crucial for the success of any experiment. For this purpose, we relied on hardware provided by **National Instruments (NI).** A summary of devices used are as follows:

3.5.1. NI cDAQ 9174 Chassis

The DAQ chassis is a modular device on which different NI provided hardware can easily be mounted. A total of four devices can be mounted and a streamline input and output are possible using only one USB port which goes into the computer.

Figure 9 NI cDAQ 9174 Chassis

3.5.2. NI 9219 Analog Input Module

This NI instrument is a multipurpose data reading device with a range of measurements from current, Voltage, strain, temperature, etc. The sensors compatible with this device range from RTDs, thermocouples, strain gauges and other powered devices. You can setup any sensor with this device using many calibration techniques[7][20].

Figure 10 NI 9219 Analog Input Module

3.6. Pulse Width Modulation

Pulse width Modulation (PWM) breaks a DC signal into pulses at regular intervals. The value of PWM ranges from 0 to 1 with which the *on/off* time of a pulse is controlled. More the value of PWM, more is the time for a pulse to stay in the *on state*. PWM is used as an input into the SMA springs as analog signal does not pass through a coil and a straight DC input might damage the Spring. For this purpose, the following devices are used:

3.6.1. Arduino Uno

Arduino Uno is a small microcontroller with 14 digital I/O pins, and 6 analog inputs. It is used for small projects and is programmed by C++ language. It is easy to be used with a computer with which a program is written and stored in the Arduino. The Arduino executes the program on its

own as a stand-alone microcontroller. For this project the Arduino is used as an on/off switch and a PWM regulator.

Figure 11 Arduino Uno

3.6.2.L298n Motor Driver

It is a device used with Arduino to control the speed and direction of motors. There is one voltage input, two outputs of phase 180^{o} to each other. Signals from Arduino reach the driver and it acts as a PWM driver which changes the direction and speed of motors. In this project this driver is used to execute the PWM commands given by the Arduino translated in the voltage available at the driver.

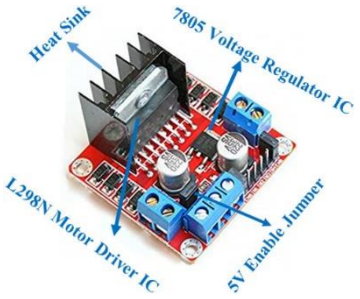

Figure 12 L298n Motor Driver

CHAPTER 4: SOFTWARE DEVELOPMENT

4.1. Introduction

In the previous chapter we discussed the hardware used for performing experiments. These hardware modules need to be passed through a software program which can collect data from and send data to these devices. For this purpose, a software needs to be developed to take all the readings and perform input and output operations. For our experiment, the software used was *NI LABVIEW 2017.*

This chapter discusses some basics of LABVIEW, and the programs developed to perform experiments for this thesis.

4.2. LABVIEW 2017

LABVIEW is a graphical programming language developed for engineers and scientists. It removes the problem of writing long sequential codes like other text-based languages. The operations performed and the code execution can be monitored in real time. It makes debugging easy for a user as he can visualize the results as the program is running.

4.2.1. Virtual Instruments (VIs)

LABVIEW programs are called VIs because their operations are like a physical instrument like an oscilloscope and multimeters. A wide set of tools is available for different operations like taking data, analyzing, displaying, and storing results.

A VI has three basic parts:

1. Front Panel
2. Block Diagram
3. Icon and Connector Palette

4.2.1.1.Front Panel

The front panel is the user interface built to by the user to give *controls and indicators* of the program for operation.

Controls are the inputs to a program. In math terms controls can be called the input variables. These include dials, knobs, on/off buttons, and input numbers/arrays.

Indicators are the outputs from the program. These show the results of a process during and after the execution of a program. These include graphs, LEDs, and other graphical/numerical results.

Icon Palette in the front panel contains all the controls and indicators that can be utilized for the user interface construction.

A front panel of VI with Icons Palette is shown below:

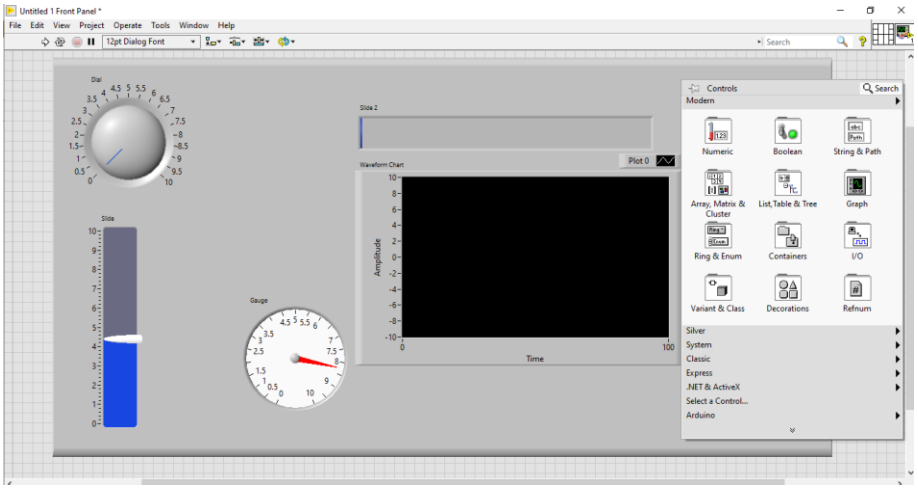

Figure 13 Front Panel with Controls, Indicators and Icon Palette

4.2.1.2.Block Diagram

Once all the controls and indicators are set up in the front panel for the user to work with, the real process of building a program starts in the block diagram. The block diagram contains the information about how the controls and indicators work in a program.

The block diagram contains a vast set of mathematical and logical operations that can transform an input to output. Different programs related to controls, measurements, instrumentation, signal processing, statistics, and other data operations can be utilized to build complex programs.

The **Icon/connector Palette** in block diagram contains all the sets of operations discussed above. Block diagram is the brain of the program. All the debugging operations are performed in this part of the LABVIEW VI.

A block diagram with connector Pallets is shown below:

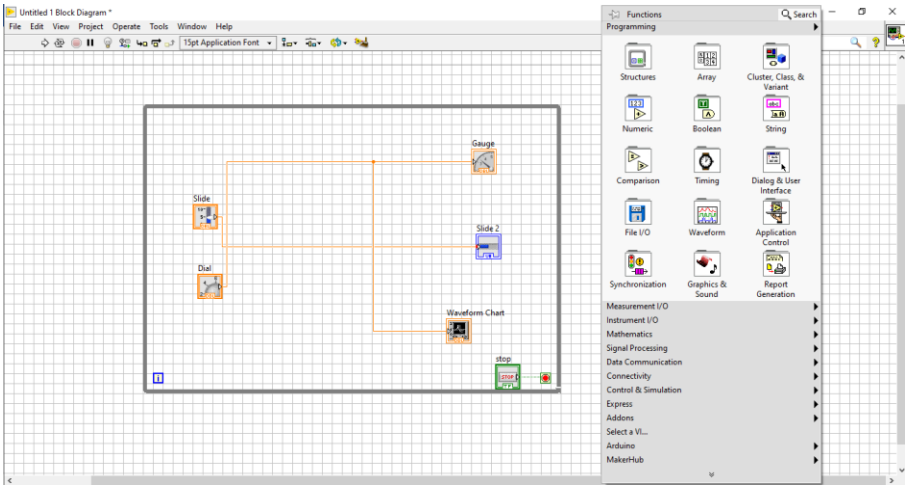

Figure 14 Block Diagram with Connector Palette

4.3. Experiment Design

The main purpose of this thesis was to control the position of Shape Memory Alloy spring using PID algorithm. Different experiments were designed in LABVIEW for the purpose of gathering data to analyze the behavior of spring to controlling its position. These are discussed below:

4.3.1. DAQ Assistant Express VI

The DAQ assistant is a module in LABVIEW used to gather data from different sensors connected with NI devices. By placing DAQ assistant in a VI we can choose the data to be read by different sensors at the frequency that we define. The DAQ Assistant module is shown below:

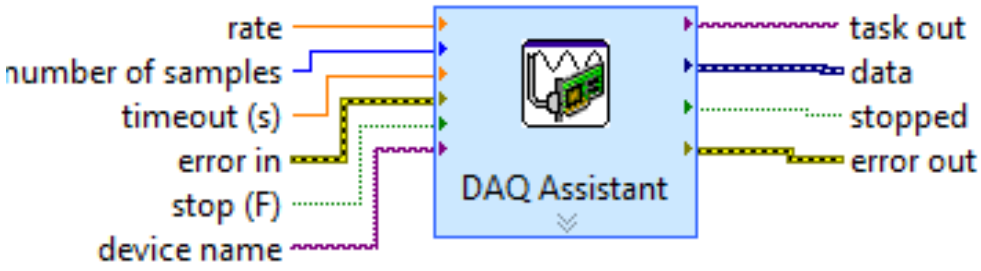

Figure 15 DAQ Assistant Express VI

Once placed in a VI we open the interface by double clicking the *DAQ assistant*. It opens a separate express VI in which different options are given for input/output of data. For our thesis we are obtaining the readings of current and LVDT from our NI 9219 Analog Input module. The DAQ assistant interface looks as follows:

4.3.2. Arduino Integration

It must be noted that Arduino is not naturally compatible with LABVIEW and needs a firmware to be installed into the program for a successful Integration. For this purpose, LINX firmware by LABVIEW Makerhub was used. The LINX palette in a VI is shown below:

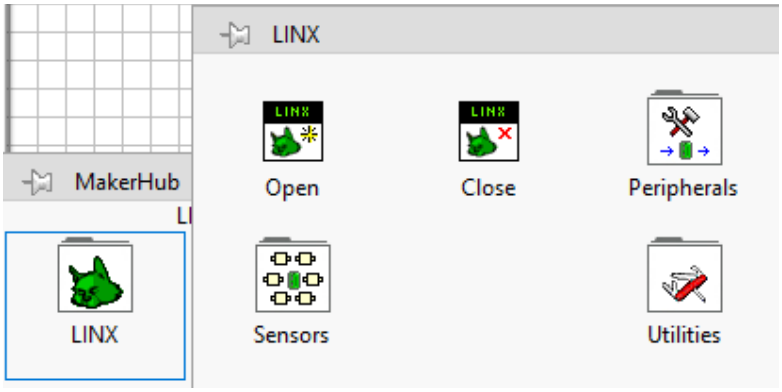

Figure 16 LINX palette for Arduino LABVIEW Integration

4.3.3. Optimal Voltage for operation

The program devised to measure the optimal voltage involved the use of basic modules such as Arduino, HC-SR04 and L298n driver. The front panel and block diagrams of this experiment are shown below:

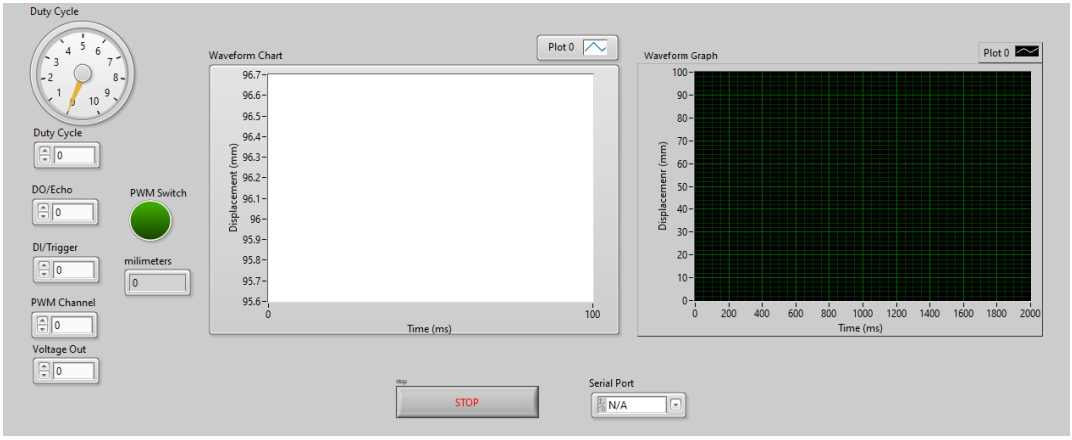

Figure 17 Front Panel Optimal Voltage measurement

A waveform chart is used in the front panel to monitor the displacement produced at different voltages as the process is carried out. Once the program ends the data of whole process is transferred to a waveform graph which can be copied to be processed as an excel sheet.

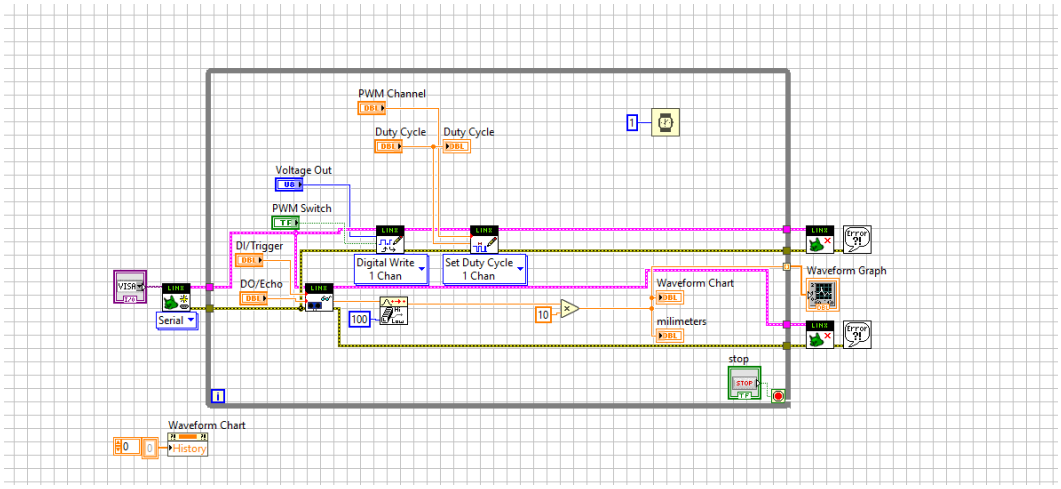

Figure 18 Block Diagram Optimal Voltage measurement

In the block diagram above the controls and indicators in the front panel are connected to form a program that makes the logic of whole operation. There is arithmetic, logical, statistical and other processes being carried out all at once.

4.3.4. Load Bearing Capacity of SMA spring

We devised a mechanism to add dead weights to the Nitinol spring to measure its load bearing capacity both in austenite and martensite phases. For this purpose, an additional component of data reading was included which dealt with the measurement of current around the SMA coil. The LABVIEW VI for this purpose is shown below:

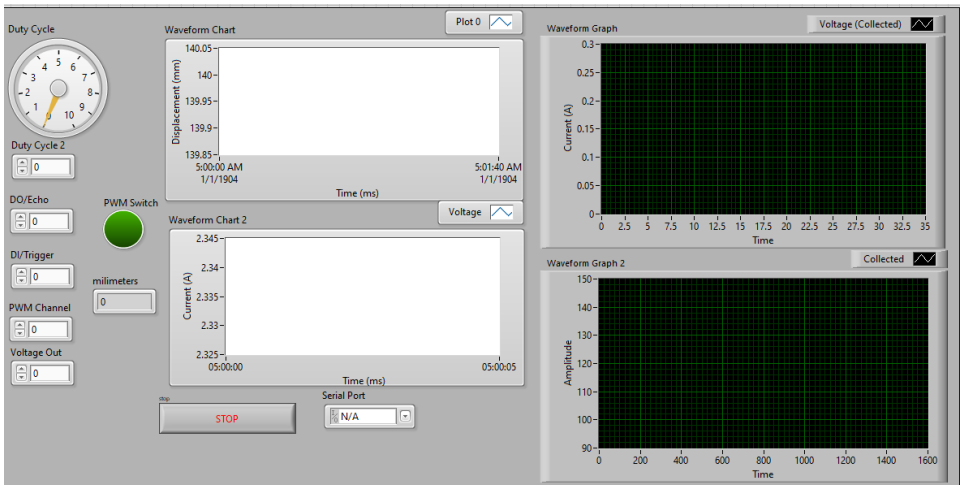

Figure 19 Front Panel Load Bearing Capacity measurement

The front panel shows two waveform charts that show current and displacement while the program is being executed. A new program runs once a new weight is added and all the data is projected on the two waveform graphs at the end of each program.

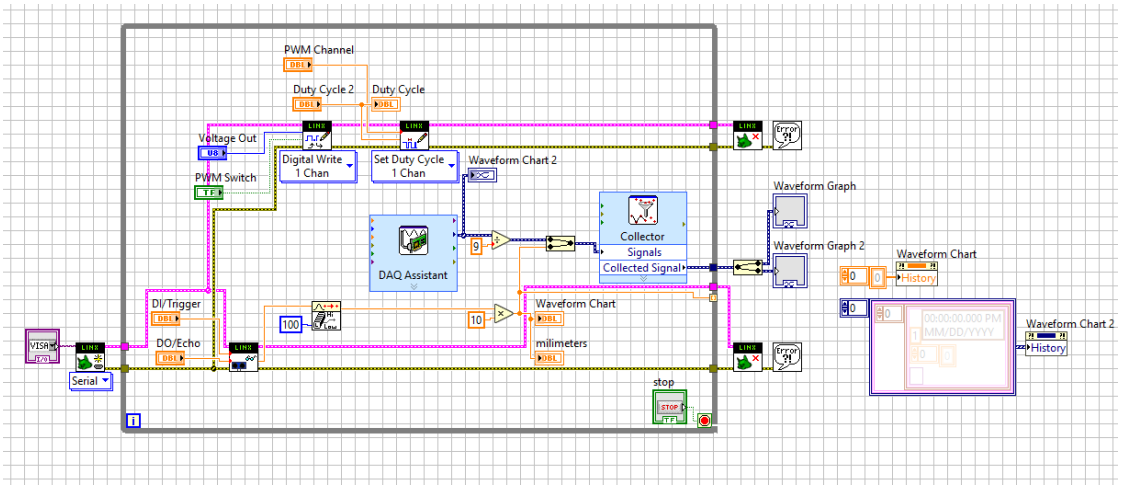

Figure 20 Block diagram Load bearing capacity measurement

The block diagram has a DAQ Assistant for the measurement of current during the execution of program. A collector expresses VI is added in the program to collect the real-time data and project on the waveform graph at the end of each experiment.

4.3.5. Displacement measurement using LVDT.

For the purpose of better data collection LVDT has been used in the experiment and its readings calibrated. This is achieved by developing a new VI as shown below:

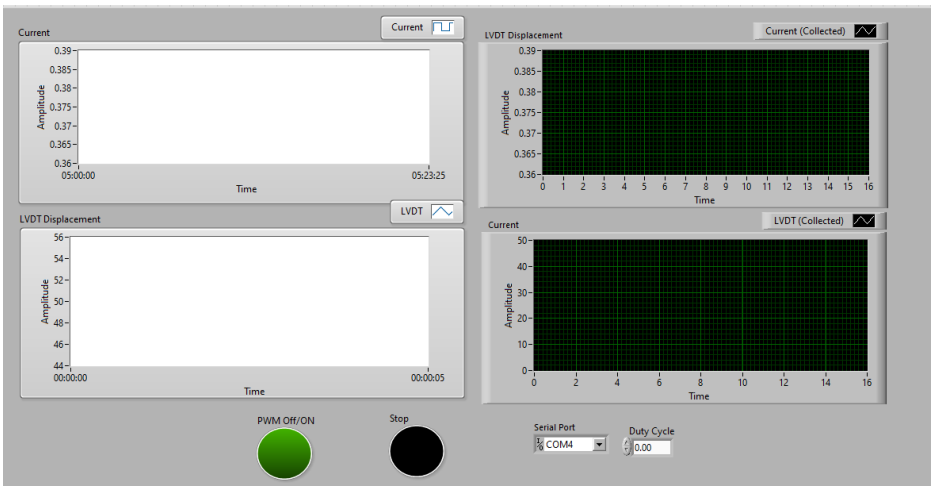

Figure 21 Front Panel of LVDT integration VI

In the above front panel the displacement charts are shown by LVDT displacement and current chart stays the same as the previous VI. The rest of the operation stays the same.

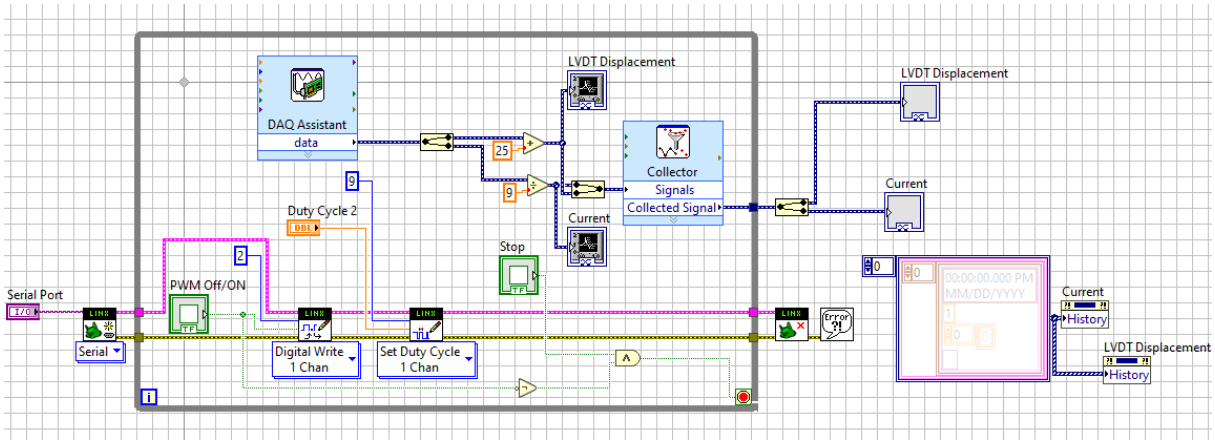

Figure 22 Block Diagram of LVDT Integration VI

The block diagram is almost the same as the VI for previous experiment. The inclusion of LVDT gives much more accurate values as compared to *HC-SR04 ultrasonic sensor* used in the previous experiments.

4.3.6. PID algorithm for position control

A program was developed for the control the positioning of Nitinol spring using the traditional PID (Potential Integral Derivative) controller. The VI for this program is shown below:

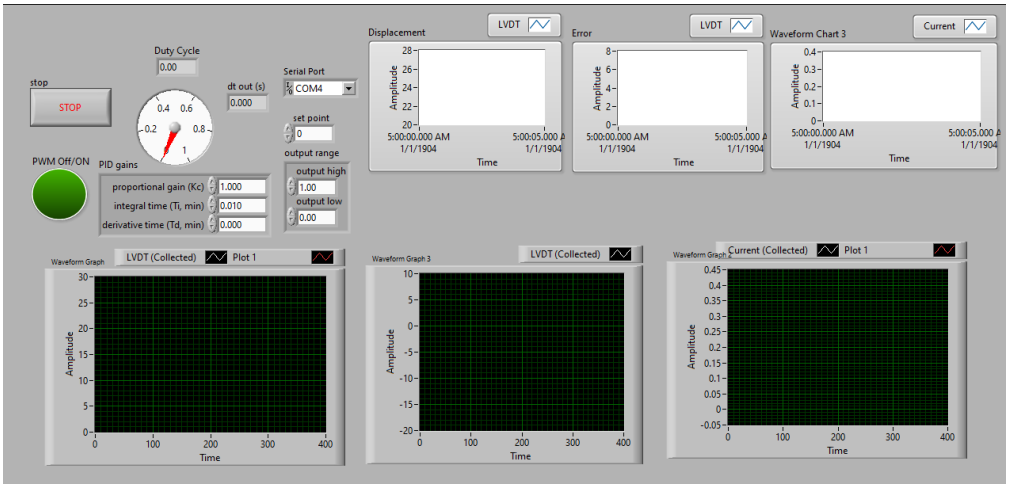

Figure 23 Front panel PID Control Algorithm

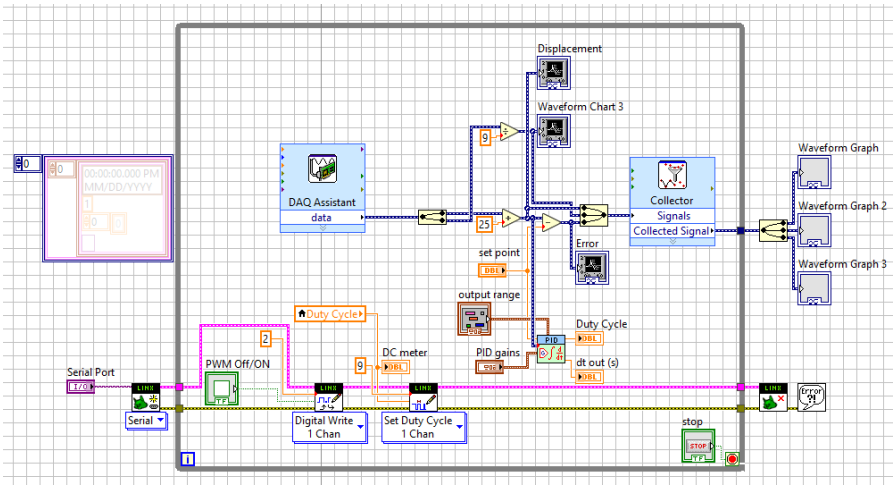

Figure 24 Block Diagram PID control Algorithm

The PID algorithm uses potential integral and derivative controls which are varied by the user to get best results.

4.3.7. Advanced PID algorithm for position control

Advanced PID algorithm is used to give the user some extra control over the program, the number of control variables is increased, and the process tends to have better performance. The advanced PID VI is shown below:

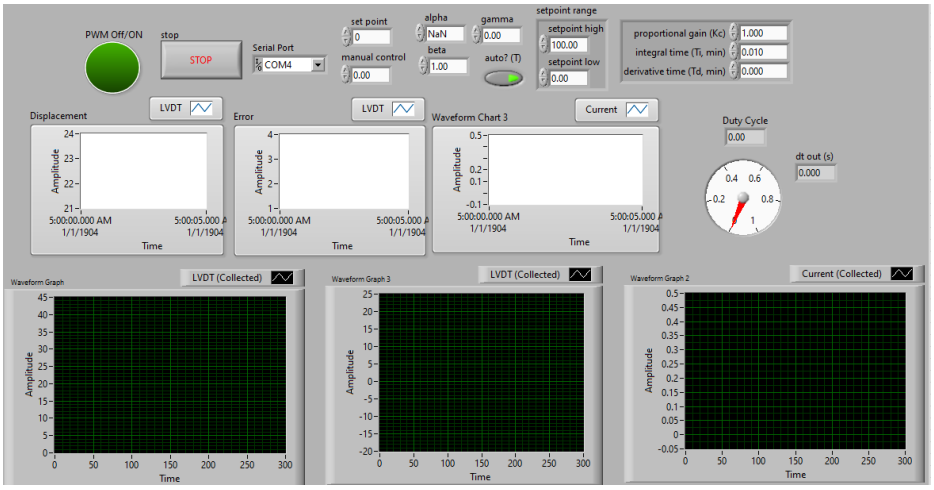

Figure 25 Front panel Advanced PID VI

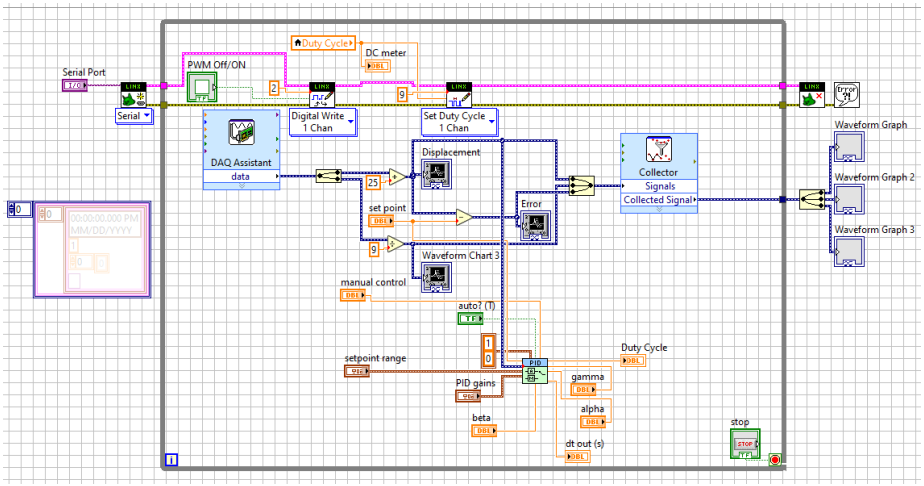

Figure 26 Block Diagram Advanced PID VI

The advanced PID uses variables like alpha, beta, and gamma in addition to the conventional PID controller to help smooth the process.

A PID control toolset user manual is provided by National Instruments which covers all the techniques used here in detail[21].

CHAPTER 5: EXPERIMENTATION AND RESULTS

After developing test bench and planning the software development, different experiments were conducted to test and examine the properties of the Shape Memory Alloy Nickel Titanium Springs. A step-by-step approach was carried out in order to get desired results of our experiments. As discussed in the introduction the objectives were carefully identified and results precisely plotted.

5.1 Finding the Optimal Voltage of Operation

For our first experiment we compared the time and path taken by the SMA spring to retract back to its original state once deformed under constant load of 10 grams while changing the input voltage in each experiment.

The difference of input voltage and voltage across SMA is explained in the table below:

Input Voltage	Voltage Across SMA wire
10 V	7.5 V
12 V	9.7 V
15 V	11.4 V
17 V	13.02 V

Table 3 Input Voltage Vs Voltage Across SMA wire

The following graph shows the displacement/contraction of SMA spring during this experiment:

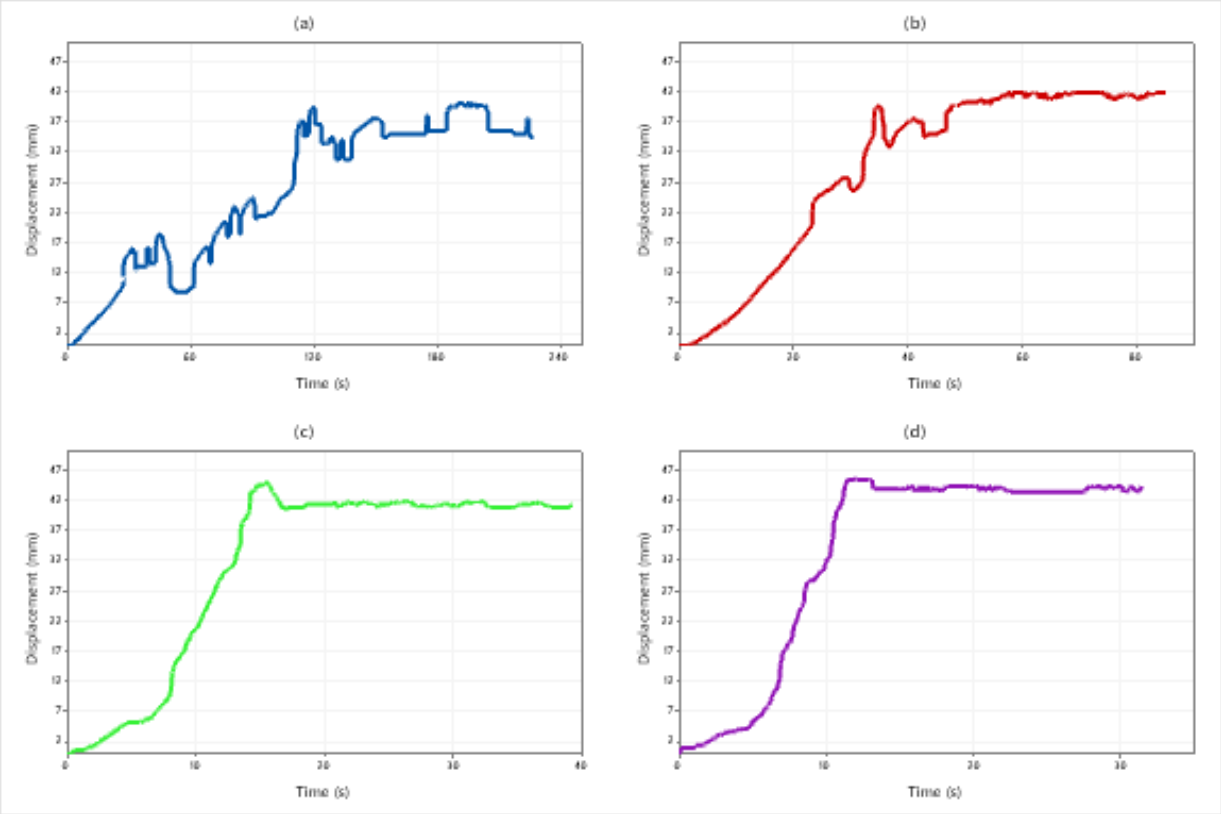

Figure 27 Displacement VS Time (at constant 10g load) for different Input Voltages
(a) 10 Volts (b) 12 Volts (c) 15 Volts (d) 17 Volts

From the graph we can clearly see that as the voltage increases across the spring the time to contract to original length is reduced. The goal here is to identify the best voltage that can be applied across the spring for uniform and at the same time fast contraction.

For the initial inputs of 10 and 12 Volts the rate of contraction is not only slow but is non-uniform. This non-uniform contraction/displacement is not ideal for many experiments. In case of graphs (c) and (d) the contraction is quite uniform. Hence, it is advised to use the input voltages high and in future experiments the input voltages shall be kept equal to or above 17 V.

5.2Testing Load Bearing Capacity

The next experiment was to find the load bearing capacity of Nitinol spring. For this experiment the spring was loaded after each experiment and the displacement and current was observed. The load was progressively increased starting from 10g up until 50 grams. Displacement as well as current was observed during each experiment. The results were later compared to understand martensitic and austenitic elongations of the spring under five different loads. Input voltage set at 20 Volts.

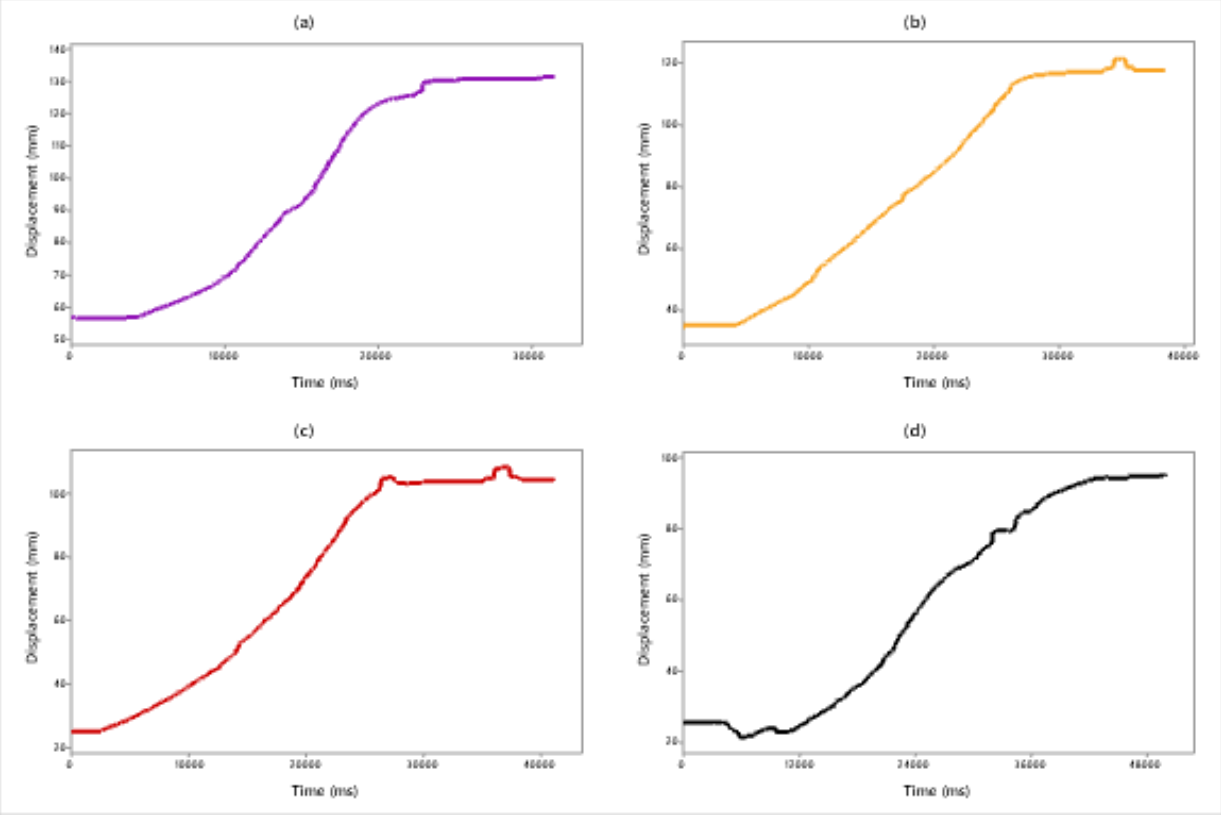

Figure 28 Displacements under varying loads (a)20g (b)30g (c)40g (d)50g

As seen from the graphs the spring had the capacity to lift the loads with minimal increase in time of lift (response time) as the weights increased. As moving from 20g(a) to 50g(e). The elongation

is increased. The spring does not retract back to its original form, however, the amount of displacement produced is almost the same (47.5mm approx.).

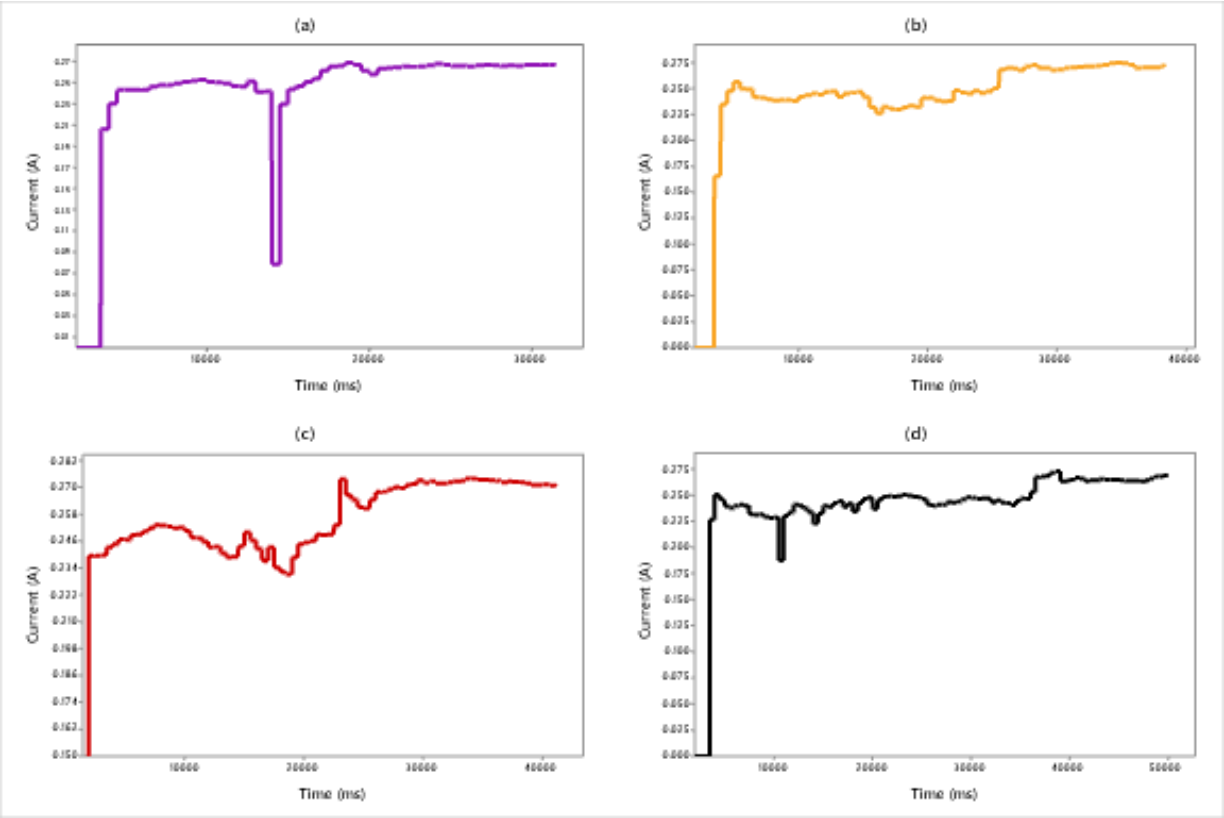

Figure 29 Currents at different Loads (a)20g (b)30g (c)40g (d)50g

The currents were also compared for each of this experiment which, as seen in the graph, show similar maximum values. For 20g(a) and 50g(d) load the maximum observed current reaches approximately 0.275A. But as the load increases the frequency of current oscillations also increase, which could be the result of overheating at smaller loads.

Lastly during this experiment, the starting (martensitic loading) and finishing (austenitic loading) displacements were observed while taking the 10g finishing displacement (austenitic load) as the reference for others to compare from.

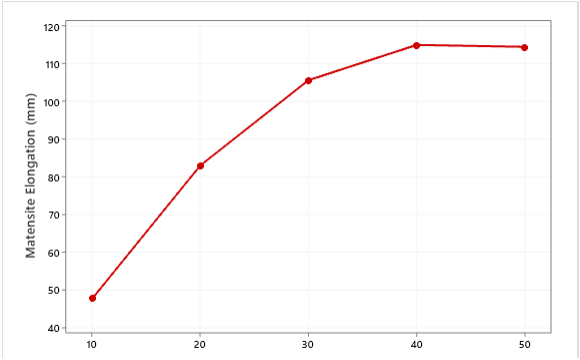

Figure 31 Elongation Vs Load (Starting Displacements)

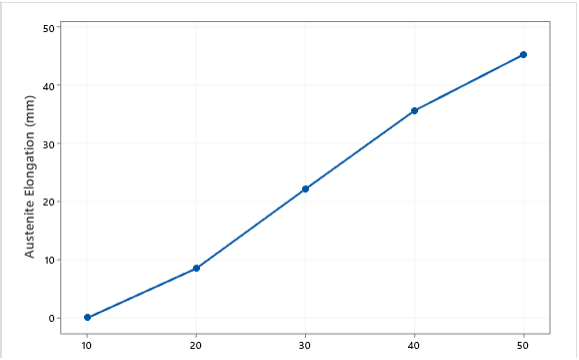

Figure 30 Elongation VS Load (Finishing Displacement)

The above graphs show how load affects elongation in martensite and austenite state. Interestingly, the spring does not regain its original shape when heated as the weight increases. The reason is that the Young's modulus in Austenitic phase is greater than martensitic phase and hence the elongation is smaller above Austenite finish temperature A_f. However, the displacement (contraction) remains the same as discussed above.

5.3 PID Position Control Mechanism

A PID algorithm is built to control the position of SMA spring. The objective is to use different techniques to optimally position the spring and minimize error. The following table gives the conditions under which the experiment is performed:

Input Voltage	22 Volts
Set Point	20 mm
Controller	P, PI, PID, PID advanced

Table 4 Experimental Conditions SMA position control

5.3.1 P Controller

At first the P controller is used to understand the extent of error generated using simple algorithms. Multiple runs are performed, and the best results generated are used in the study. For this experiments the best result are observed at K=0.4 while all other values like T_i and T_d are kept zero. The results are shown below:

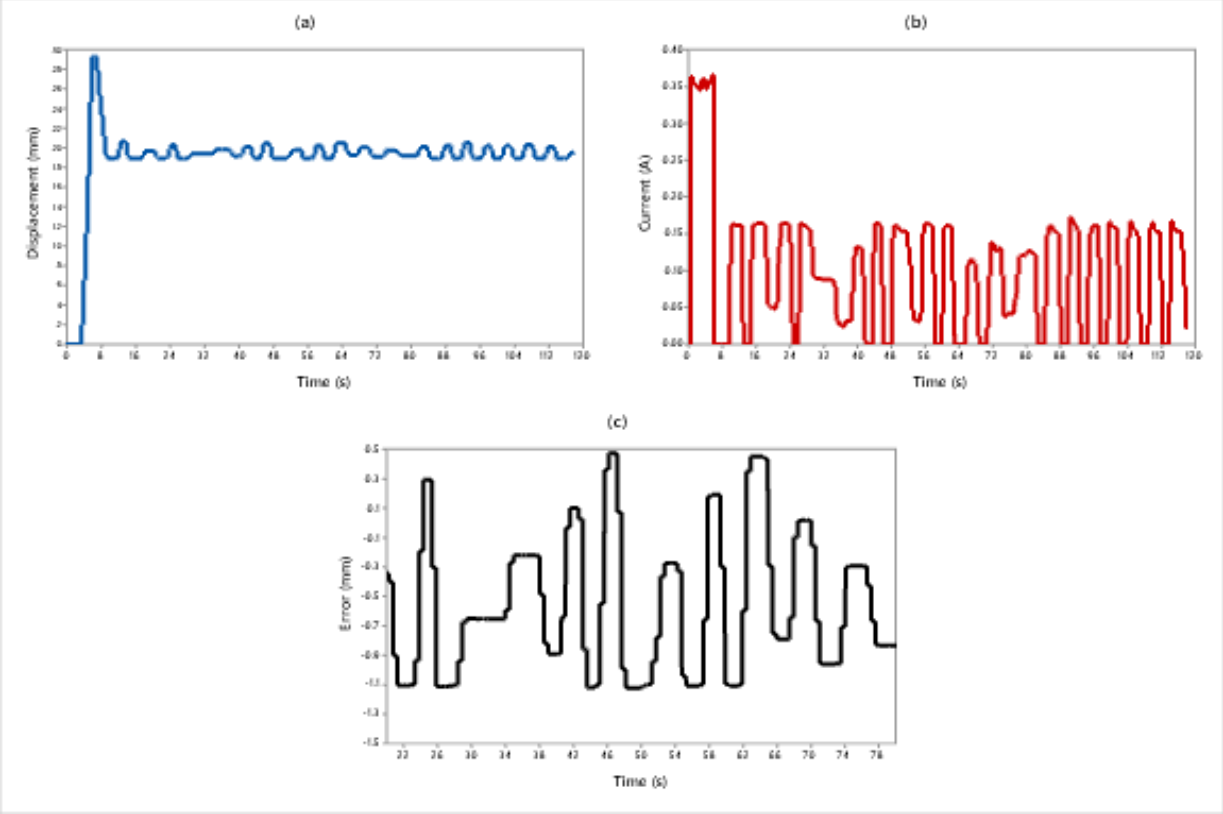

Figure 32 P controller K=0.4 (a)Displacement(b)Current(c)Error

As seen from the figure 32(a) the displacement starts around 5 seconds, and a sharp rise is observed. There is an initial overshoot of around 8mm before the algorithm adjusts to the increase in displacement and starts to lower the current input as observed in figure 32(b). The system goes smooth, and the error is reduced considerably. A pattern is formed where in the rise and fall of displacement stays consistent around the setpoint (20mm). An error between -1.1mm and 0.5mm is seen to stay consistently oscillating as the time goes on. This error is shown in the figure 32(c) which is taken during the interval 20s to 80s of time. The P-controller gave a result that is much better than expected and goes to show that with better tuning procedures and the use of PID controller can result in good macro-level controls of shape memory alloy springs.

5.3.2 PI Controller

Based on the results produced during the testing using P-controller, the next step was to use PI controller and find out the best combination to attribute good control of SMA spring movement and positioning. Several combinations were tried and compared for errors and the best results produced are shown in the following figures. The setpoint is 20mm while the input voltage is kept at 22 volts. The best combination was found at K=10 and T_i=0.2. The figure below gives the results observed during the experimentation:

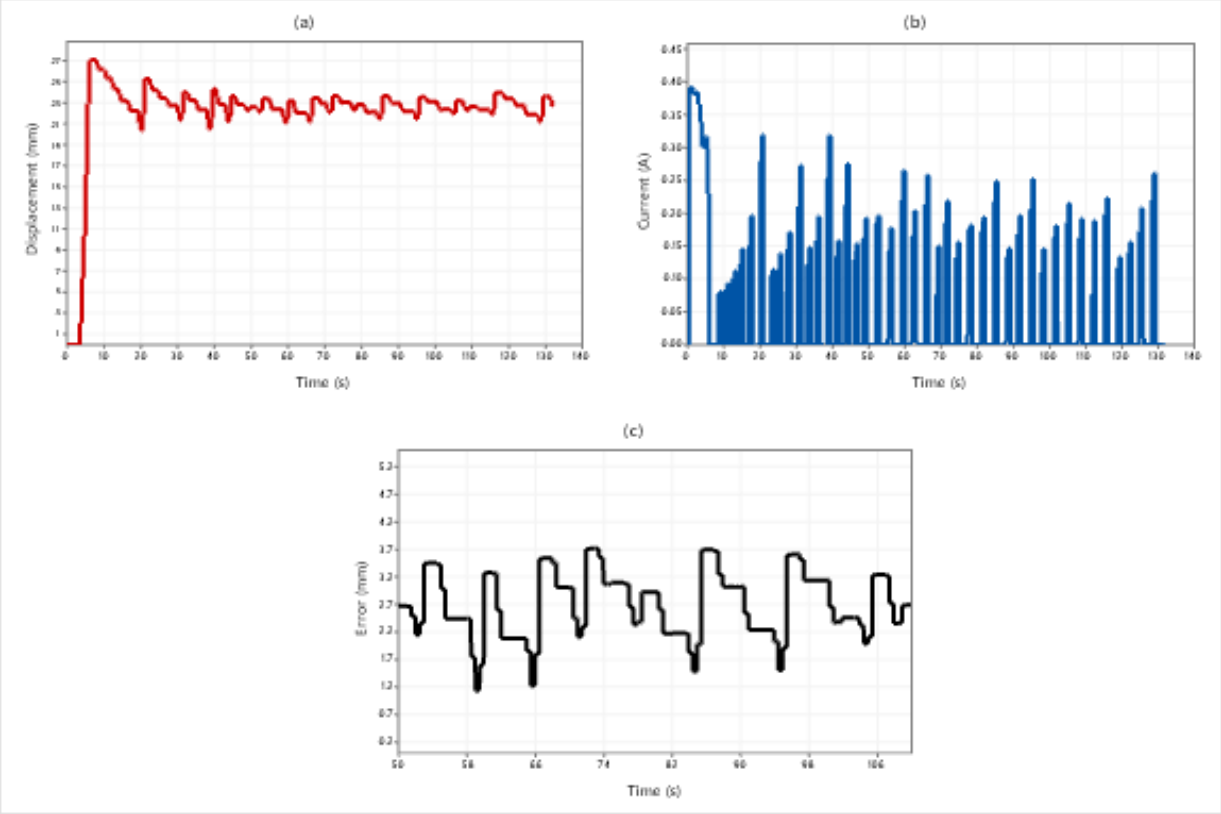

Figure 33 PI-controller (a)displacement (b)Current (c)error

The displacement produced is shown in Figure 33(a) which starts at around 5 seconds and rises quickly peaking at 27mm. This shows a small rise time but a big overshoot as a result. The controller seems to kick in to control the flow of current and the oscillations start to grow smaller as the time moves on. This is evident from the figure 33(b) showing the flow of current in real-

time as the displacement changes. There are evident spikes in currents and as a result the displacement is increased subsequently. Figure 33(c) shows the error in the observation when the oscillations are smoothened overtime, and no big change is observed. We can see a constant error between 0.8mm and 3.7mm during the process with a mean of 2.25mm.

5.3.3 PID Controller

The next set of experiments consisted of using all variables in a PID algorithm. Like the experiments performed above, the best combination of variables was observed using hit and trial method. A number of different conditions were tested and the conditions for a good set up was observed at K=10 T_i=0.2 and T_d=0.05. The results are plotted in the form of graphs as observed below:

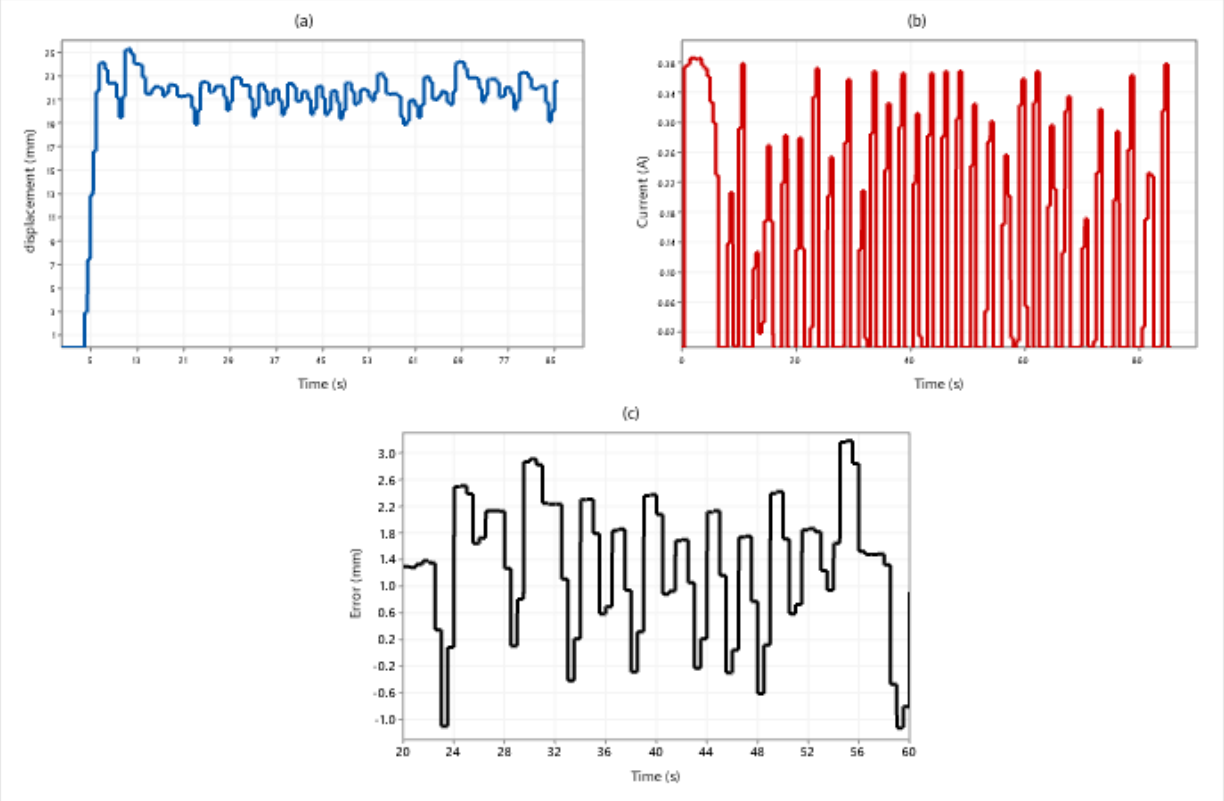

Figure 34 PID Controller K=10 Ti=0.2 Td=0.05 (a)displacement(b)Current(c)error

Figure 34(a) shows the displacement produced during the PID position-controlled process. As the process starts the displacement rise is abrupt and completes within 1 second while starts at 5 seconds after the start of experiment which is due to the time it takes to heat the SMA spring to its transition temperature. This can also be observed in figure 34(b) as the current peaks at 0.38 Amps and starts to come down again as the controller starts to control the movement. The setpoint is set at 20mm of displacement. The overshoot is around 25mm after which the displacement rises again to 26mm and then starts to die down and position control starts to take effect. For this experiment the displacement is observed not be smoothed but random at many intervals. For this reason, there

is no regular pattern as can be seen in the error graph of figure 34(c). The error observed is seen between -1.3- and +3.4mm.

The three PID algorithmic experiments performed show different possibilities of controlling the experiments. These experiments are also compared side by side to understand which combination can be used in different industries. The overview of the above experiments is explained below:

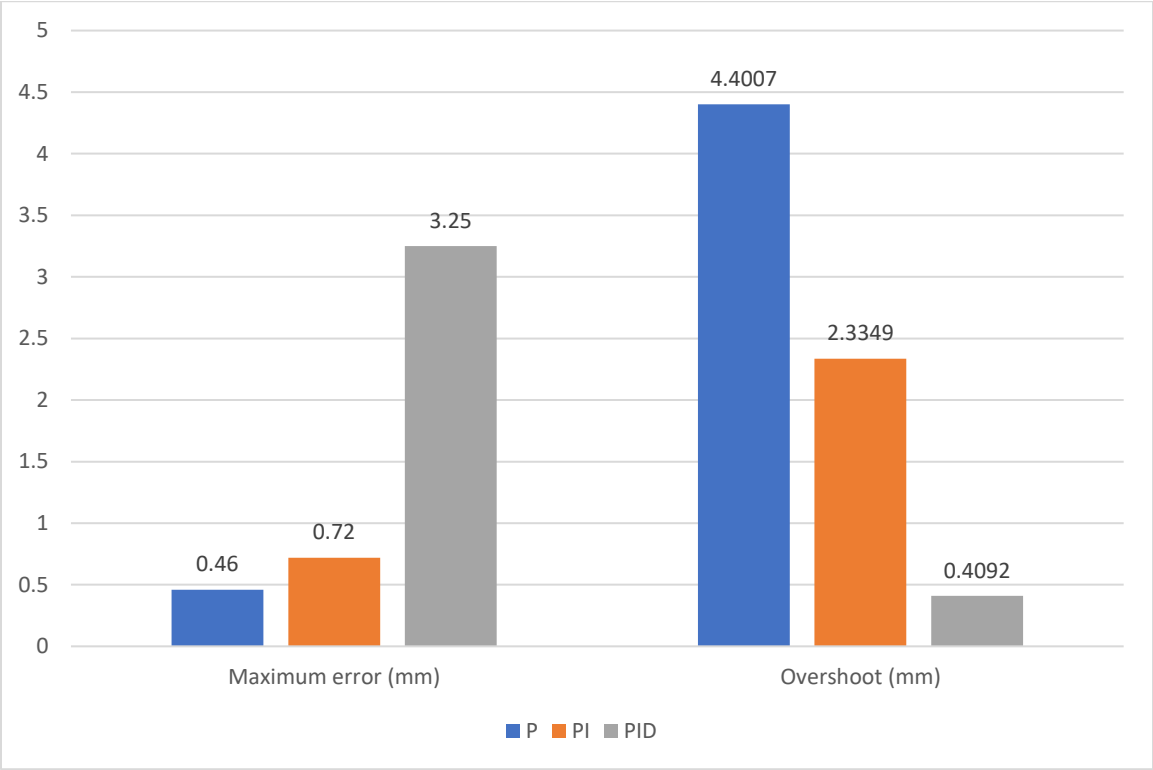

Figure 35 PID experiments Results overview.

From the above figure 35 it can be concluded that least error is produced while using the P-controller alone, this is true because the controller value was kept below 1 and minimum error was produced due to low amount of current flowing through the material, while the overshoot is produced at a maximum value which seriously compromises its performance. Conversely, while using PID controller the amount of overshoot is reduced considerably with a very low value as compared to P-controller but produces a very high error in comparison.

It can be concluded that depending upon the use and value of errors produced a compromise must be made while choosing the best controller for a particular application. A middle ground can be established by using PI controller which has a low maximum error and a workable overshoot compared to both P and PID controllers.

5.4 Advanced PID Controller

Advanced PID controller gives extra control to the existing PID algorithm and control practices are improved as a result. For this controller, an addition of variables like beta, gamma and alpha is introduced. Various tests were performed to minimize the error and the overshoot that is observed during the process. The process was narrowed down to two possible combinations that resulted in better performance. These are discussed as follows:

Using β Variable, the experiments were performed, and a good pattern was observed using the values as k=10 T_i=0.2, T_d=0.01, and β=0.2. The results of this experiment are shown below:

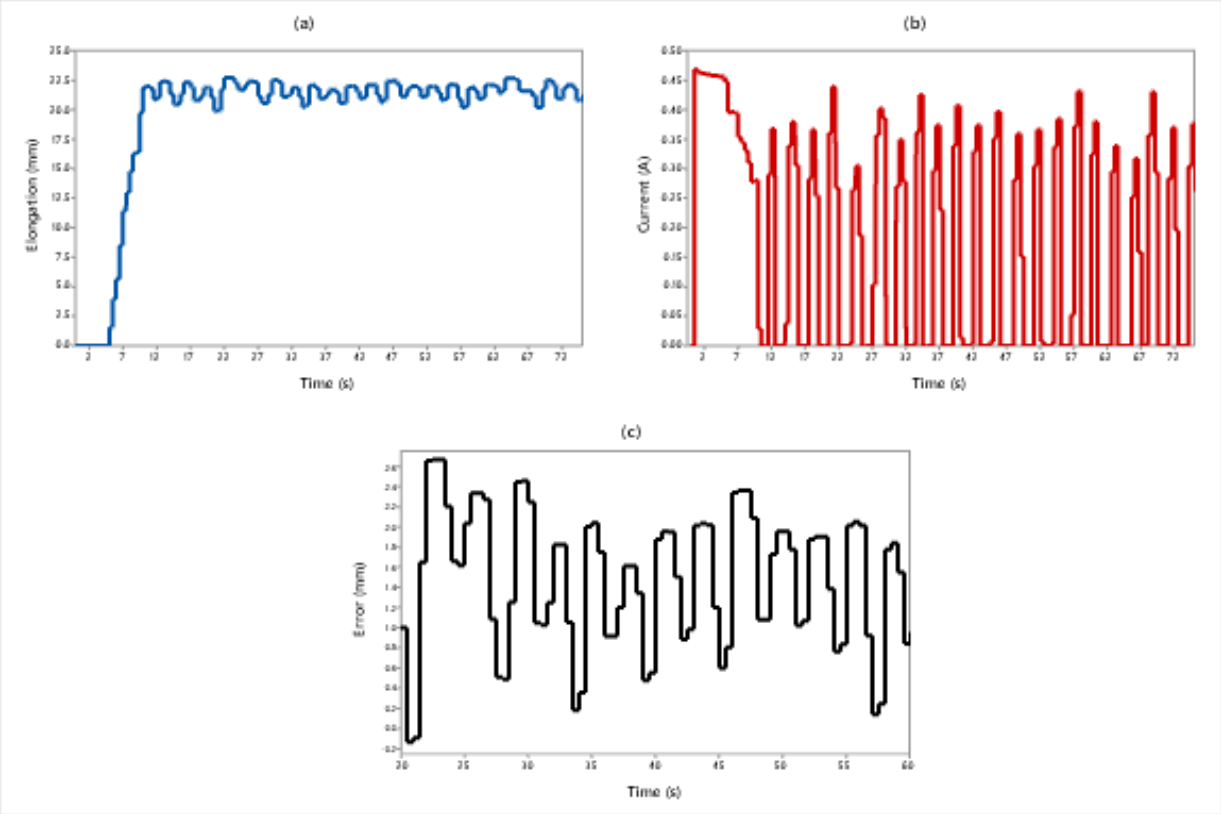

Figure 36 Advanced PID algorithm β=0.2 (a)displacement (b)current (c)error

The results of the above process show a slow rise as compared to traditional PID algorithm. Figure 36(a) gives the displacement curve which shows a rise time of around 8 seconds and overshoot of 22.5mm while the setpoint was kept at 20mm (2.5mm error). The process has been smoothed quite quickly to produce a constantly oscillating error.

Figure 36 (b) gives the current input into the SMA which is also constantly changing with a maximum current at the beginning of the experiment at 0.4339A. The quick smoothening of displacement curve also results in a constant error graph in figure 36(c). The error starts at a max value between -0.126mm and 2.67mm and eventually reduces to a constantly changing range of 0.211mm and 2.38mm.

Using β and γ variables, the process is observed using multiple test runs and satisfactory results were plotted at K=10, T_i=0.2, T_d=0.01, β=0.5 and γ=0.1. Figure 37 contains the graphs representing the performance of SMA spring under these conditions.

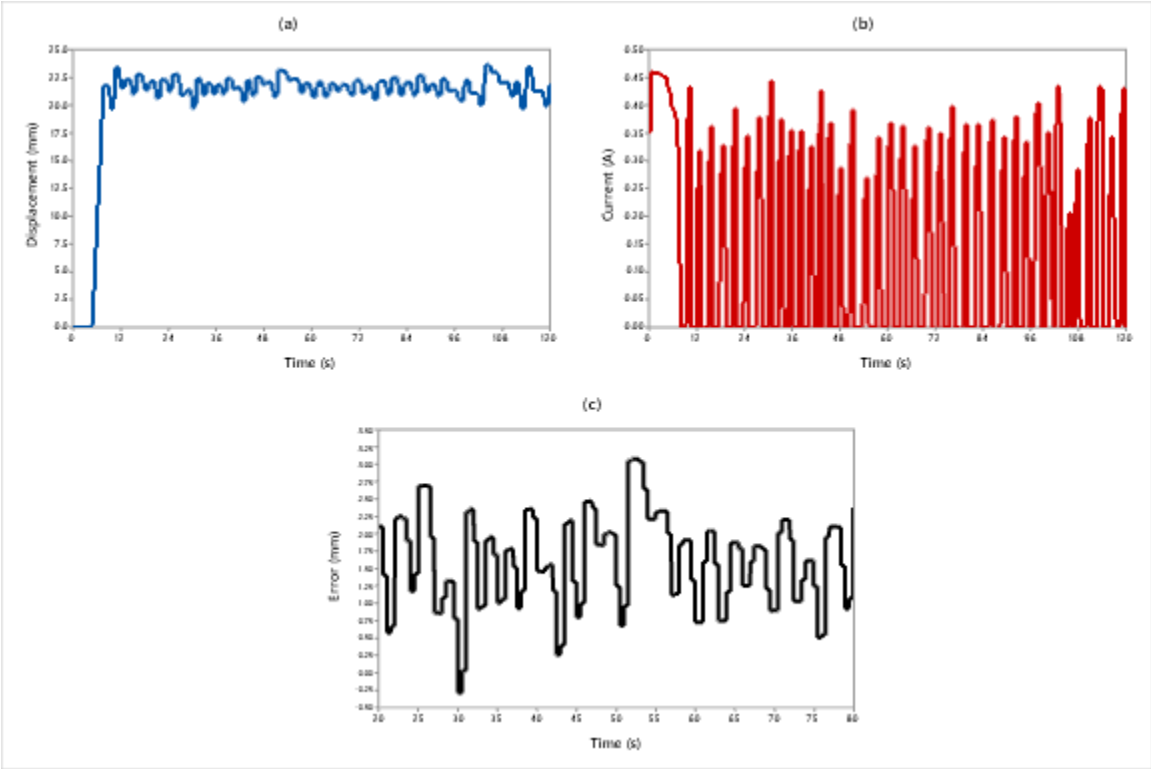

Figure 37 PID Advanced β=0.5, γ=0.1 (a)displacement (b)elongation (c)error

Figure 37(a) shows the displacement increased from the start of the process a slower rise time and a very small overshoot reaching up to only 21.8344mm (error of 1.8344mm) but at the next oscillation the displacement is increased due to overcompensation by the controller. The graph is again quickly streamlined and constant oscillations start to emerge. The current in figure 37(b) also shows a much smoother on and off characteristic with maximum value only reaching at the beginning of the experiment at 0.459A. Similarly, in figure 37(c) the error is seemingly oscillating between -0.266mm and 3.08mm at the extremes and as the time goes reducing to the range of 0.52mm and 2.205mm.

In comparison to PID controller the Advanced PID algorithm has an advantage in reducing the overshoot and a quick response while reaching a smooth pattern in oscillations of error. While the PID controller gives a sharp rise to reach the max value, the advanced PID compensates the time lost with better performance as the time moves on. If the goal of application is to minimize error and reduce overshoot as compared to fast response the Advanced PID algorithm should be preferred over simple PID control.

CHAPTER 6: CONCLUSION AND FUTURE RECOMMENDATIONS

6.1 Conclusion

In this thesis an introduction to shape memory alloys, particularly Nitinol (NiTi) was discussed and literature behind was reviewed. An experimental rig was built to test the properties of Nitinol and its behavior under different loads was observed. A software program was created to carry out the experiments at different working conditions. The goal was to understand the properties of the special material and different ways were employed to control the position of the SMA spring. The thesis discussed the already available programs used widely in industry to control the position of actuators. The controllers used were PID (potential, integral, derivative) controller and Advanced PID controllers. The results were generated and discussed thoroughly to find an understanding of the subject in hand.

The SMAs are unique in their properties and hard to control by simple mechanisms but using available ready to use processes like PID can definitely prove to be helpful to reach some level of position control and hence can be applied in industries that do not rely heavily on precision applications. The results observed from this research point out that these materials are extremely durable and have high weight bearing capacity. The spring used was able to generate maximum displacement at loads higher than 10 times its own load. The PID controller was able to perform position control with a maximum accuracy of up to 0.46mm while the lowest overshoot of 0.4092mm was observed but a sacrifice had to be made between desired error reduction and overshoot amount. The Advanced PID algorithm showed promise reducing both the overshoot and error at the same time with minimum overshoot of 1.8344mm and minimum error range of 0.211mm and 2.38mm. Overall the process was observed to improve overtime as the experiment continued.

6.2 Future Recommendations

There are still many off the shelf programs that can be employed to control the position of SMA actuators which should be tested. These are easily found and implemented in programs like LABVIEW which has been the central part of this thesis.

The algorithms recommended for future experiments are:

a) PID autotuning algorithm

b) Advanced PID autotuning algorithm

c) Fuzzy Logics and many others

References

[1] J. Mohd Jani, M. Leary, A. Subic, and M. A. Gibson, "A review of shape memory alloy research, applications and opportunities," *Mater. Des.*, vol. 56, pp. 1078–1113, Apr. 2014.

[2] C. Naresh, P. S. C. Bose, and C. S. P. Rao, "Shape memory alloys: A state of art review," *IOP Conf. Ser. Mater. Sci. Eng.*, vol. 149, no. 1, 2016.

[3] N. . Morgan, "Medical shape memory alloy applications—the market and its products," *Mater. Sci. Eng. A*, vol. 378, no. 1–2, pp. 16–23, Jul. 2004.

[4] J. Van Humbeeck, "Non-medical applications of shape memory alloys," vol. 275, pp. 134–148, 1999.

[5] L. Petrini, F. Migliavacca, P. Massarotti, S. Schievano, G. Dubini, and F. Auricchio, "Computational studies of shape memory alloy behavior in biomedical applications," *J. Biomech. Eng.*, vol. 127, no. 4, pp. 716–725, 2005.

[6] W. Huang, "On the selection of shape memory alloys for actuators," no. June 2000, pp. 11–19, 2002.

[7] P. Senthilkumar, G. N. Dayananda, M. Umapathy, and V. Shankar, "Experimental evaluation of a shape memory alloy wire actuator with a modulated adaptive controller for position control," *Smart Mater. Struct.*, vol. 21, no. 1, 2012.

[8] E. Asua, V. Etxebarria, and A. García-Arribas, "Neural network-based micropositioning control of smart shape memory alloy actuators," *Eng. Appl. Artif. Intell.*, vol. 21, no. 5, pp. 796–804, 2008.

[9] E. Asua, V. Etxebarria, and A. Garćia-Arribas, "Micropositioning control using shape memory alloys," in *Proceedings of the IEEE International Conference on Control Applications*, 2006.

[10] P. A. Gédouin, E. Delaleau, J. M. Bourgeot, C. Join, S. Arbab Chirani, and S. Calloch, "Experimental comparison of classical PID and model-free control: Position control of a shape memory alloy active spring," *Control Eng. Pract.*, vol. 19, no. 5, pp. 433–441, 2011.

[11] K. E. Wilkes and P. K. Liaw, "Fatigue behavior of shape-memory alloys," *Jom*, vol. 52, no. 10, pp. 45–51, 2000.

[12] L. Sun *et al.*, "Stimulus-responsive shape memory materials: A review," *Mater. Des.*, vol. 33, no. 1, pp. 577–640, 2012.

[13] H. Wang, H. Y. Huang, and Y. J. Su, "Tuning the operation temperature window of the elastocaloric effect in Cu–Al–Mn shape memory alloys by composition design," *J. Alloys Compd.*, vol. 828, p. 154265, 2020.

[14] S. Barbarino, E. L. Saavedra Flores, R. M. Ajaj, I. Dayyani, and M. I. Friswell, "A review on shape memory alloys with applications to morphing aircraft," *Smart Mater. Struct.*, vol. 23, no. 6, 2014.

[15] D. Reynaerts and H. Van Brussel, “Design aspects of shape memory actuators,” *Mechatronics*, vol. 8, no. 6, pp. 635–656, 1998.

[16] A. Pruski and H. Kihl, “Shape memory alloy hysteresis,” *Sensors Actuators A. Phys.*, vol. 36, no. 1, pp. 29–35, 1993.

[17] Y. H. Teh and R. Featherstone, “Frequency response analysis of shape memory alloy actuators,” *Int. Conf. Smart Mater. Nanotechnol. Eng.*, vol. 6423, no. July, p. 64232J, 2007.

[18] S. H. Lee and S. W. Kim, “Improved position control of shape memory alloy actuator using the self-sensing model,” *Sensors Actuators, A Phys.*, vol. 297, p. 111529, 2019.

[19] K. H. Ang, G. Chong, and Y. Li, “PID control system analysis, design, and technology,” *IEEE Trans. Control Syst. Technol.*, vol. 13, no. 4, pp. 559–576, 2005.

[20] S. Simultaneous and U. Measurements, “DATASHEET.”

[21] N. Instruments, “PID Control Toolset User Manual,” *Manual*, no. 322192, pp. 1–180, 2001.